GTP-Induced Membrane Binding and Ion Channel Activity of Annexin VI: Is Annexin VI a GTP Biosensor?

Aneta Kirilenko,* Marcin Golczak,* Slawomir Pikula,* Rene Buchet,† and Joanna Bandorowicz-Pikula*
*Department of Cellular Biochemistry, Nencki Institute of Experimental Biology, 02-093 Warsaw, Poland, and †Laboratoire de Physico-Chimie Biologique, Université Claude Bernard, Lyon 1, UFR de Chimie-Biochimie, CNRS UMR 5013, F-69622 Villeurbanne, France

ABSTRACT Annexin VI (AnxVI) formed ion channels in planar lipid bilayers that were induced by the addition of millimolar guanosine 5′-triphosphate (GTP) at pH 7.4 and that were not accompanied by a penetration of the protein into the membrane hydrophobic region. GTP-influenced interactions of AnxVI with Ca^{2+}/liposomes produced small structural alterations as revealed by circular dichroism and infrared spectroscopies. Guanosine 5′-3-*O*-(thio)-triphosphate (GTPγS) binding to AnxVI, promoted by the photorelease of GTPγS from GTPγS[1-(4,5-dimethoxy-2-nitrophenyl)-ethyl] (caged-GTPγS), affected three to four amino acid residues of AnxVI in the presence of Ca^{2+}/liposomes, while about eight or nine amino acid residues were altered in their absence. This suggested that the nucleotide-binding site overlapped the lipid-binding domain of AnxVI. The binding of the fluorescent GTP analog, 2′-(or 3′)-*O*-(2,4,6-trinitrophenyl)guanosine 5′-triphosphate (TNP-GTP) to AnxVI was optimal in the presence of Ca^{2+}/liposomes, with a dissociation constant (K_d) of 1 μM and stoichiometry of 1. TNP-GTP promoted fluorescence resonance energy transfer from tryptophan residues to the nucleotide. Ion conductance and fluorescence measurements of the C- and N-terminal fragments of AnxVI indicated distinct GTP-binding properties, suggesting that the existence of the GTP-induced ion channel activity of AnxVI is associated with the flexibility of the two halves of the protein. Such structural flexibility could contribute to a molecular mechanism of AnxVI acting as a GTP biosensor.

INTRODUCTION

Annexin VI (AnxVI), M_r 68–70 kDa, is a Ca^{2+}- and pH-regulated membrane binding protein exhibiting a high level of expression in mammalian tissues, such as skeletal muscles (Schmitz-Peiffer et al., 1998) and liver (Tagoe et al., 1994), as well as in specific cell types such as hypertrophic chondrocytes and osteoblasts (Kirsch et al., 2000). Intracellularly, this protein was found in the cytosol and in association with late endosomes in rat hepatocytes (Ortega et al., 1998), in the prelysosomal compartment of normal rat kidney fibroblasts and WIF-B hepatoma cells (Pons et al., 2000), and in the LDL-containing endocytic compartment of CHO cells (Grewal et al., 2000). Such an intracellular localization of AnxVI was consistent with a postulated role of this protein in endocytosis (Michaely et al., 1999; Pons et al., 2001a) and other vesicle-mediated processes (Calvo et al., 2000), including calcification of cartilage (Kirsch et al., 2000). Observations identifying AnxVI present in lipid microdomains of the sarcolemma in smooth muscle cells (Babiychuk and Draeger, 2000) implied that AnxVI may play a regulatory role in membrane microdomain assembly, in targeting some proteins into specific membrane compartments and/or in signal transduction pathways in which various guanosine 5′-triphosphate (GTP)-binding proteins participate. The molecular mechanisms associated with such activities remain unclear.

Experimental evidence indicated that AnxVI may bind purine nucleotides in vitro (Bandorowicz-Pikula et al., 1999), although the functional significance of such a property has not yet been established. The potential abilities of AnxVI to interact with various GTP-binding proteins (Bandorowicz-Pikula et al., 2001), indispensable components of the endocytic compartment and plasma membrane, were suggestive of specific factors that are involved in the regulation of the intracellular activity of AnxVI. We propose that AnxVI/nucleotide binding may participate directly or indirectly in the regulation of functions of GTP-binding proteins (Pons et al., 2001b) or GTPase activating proteins (Chow et al., 2000). The purine nucleotide may facilitate the AnxVI-membrane interaction, as was already observed in the case of ATP enhancing the binding of AnxVI to hepatocyte plasma membrane (Tagoe et al., 1994). AnxVI/GTP interactions may elicit a molecular response to regulate functions of other proteins. In this report we describe, for the first time, that GTP in a millimolar concentration range specifically induces the formation of voltage-dependent ion channels by AnxVI molecules in planar lipid bilayers. By using a fluorescent derivative of GTP, we found that the binding of AnxVI to GTP was stimulated by the interaction of the protein with lipid membranes in the presence of Ca^{2+}. The secondary structure changes of AnxVI induced by GTP were monitored with the aid of infrared and circular dichroism (CD) spectroscopies in the presence of lipids.

Submitted October 3, 2001, and accepted for publication January 8, 2002.

Address reprint requests to Joanna Bandorowicz-Pikula, Department of Cellular Biochemistry, Nencki Institute of Experimental Biology, 3 Pasteur Street, PL-02-093 Warsaw, Poland. Tel.: 48-22-6598571 ext. 347; Fax: 48-22-8225342; E-mail: bandor@nencki.gov.pl.

0006-3495/02/05/2737/09 $2.00

MATERIALS AND METHODS

Materials

GTPγS[1-(4,5-dimethoxy-2-nitrophenyl)-ethyl] (caged-GTPγS) and 2′-(or 3′)-*O*-(2,4,6-trinitrophenyl)guanosine 5′-triphosphate (TNP-GTP) were

obtained from Molecular Probes Inc. (Eugene, OR). Nucleotides, phosphatidylserine (PS) from bovine brain, phosphatidylcholine (PC) from egg yolk, and azolectin (soybean lipids), were purchased from Sigma-Aldrich (Poznan, Poland). All other chemicals were of the highest purity available.

Purification of recombinant AnxVI

Human recombinant AnxVI, and its N-terminal-AnxVIA (residues 2–342) or C-terminal-AnxVIB (residues 348–673) fragments were expressed in *Escherichia coli* strain BI21(DE3) after induction with isopropyl-β-D-thiogalactopyranoside, and purified to homogeneity as described for AnxV (Burger et al., 1993) with small modifications. Briefly, detachment of recombinant AnxVI or its fragments from liposomes prepared from bovine brain lipid extract was achieved by incubation of the mixture with 20 mM Tris-HCl, pH 8.0, 100 mM NaCl, 10 mM EGTA, 3 mM $MgCl_2$. Liposomes were then separated from the proteins by centrifugation at 100 000 $\times$ *g* for 40 min at 4°C. Finally, the supernatant containing annexins was collected, dialyzed to 20 mM Tris-HCl, pH 8.3, 0.1 mM EGTA, and loaded onto a Q-Sepharose column for further purification. AnxVI or its recombinant fragments were eluted from the column by linear gradient of NaCl (0–500 mM NaCl): whole molecule and AnxVIA were eluted with 450–500 mM NaCl, AnxVIB with 250–300 mM NaCl. Final purification of AnxVI or AnxVIA was achieved by hydroxyapatite column chromatography. Fractions containing the respective peptides were dialyzed against 10 mM phosphate buffer, pH 7.4, 0.1 mM EGTA, loaded on a column by gravity, and eluted at pH 7.4 using a linear gradient of phosphate buffer concentrations. Both peptides were recovered in fractions eluted with 230–250 mM phosphate buffer.

Single channel recordings

The single channel activity of AnxVI and recombinant fragments was measured using the black lipid membrane method (Zampighi et al., 1985), as described in detail in Golczak et al. (2001). Planar lipid bilayers were formed with an azolectin solution in decane (20 mg/ml). The assay medium contained 10 mM Tris-Hepes buffer pH 7.4, 0.1 mM EGTA or 1.0 mM $CaCl_2$, and 200 mM KCl. AnxVI, AnxVIA, and AnxVIB were added to the *cis* chamber. The final capacitance values of the lipid bilayers ranged from 110 to 200 pF and their resistance from 1 to 5 GΩ. The current signal was measured using a bilayer membrane admittance meter, model ID 562 (IDB, Gwynedd, UK), after filtration at 0.2 kHz (low-pass 4-pole Bessel filter (Warner, Hamden, CT) and digitization (A/D converter 1401, Cambridge Electronic Design, Cambridge, UK) for off-line analysis achieved with Patch and VClamp 6.40 software (Cambridge Electronic Design).

Phase separation of AnxVI in Triton X-114 solution

The phase separation test was performed as described in Bordier (1981). AnxVI (0.2 mg/ml) was incubated in 200 μl 10 mM Tris-HCl, pH 7.4, 150 mM NaCl, and 0.5% (w/v) Triton X-114 for 15 min at 4°C. Then it was layered on 300 μl 10 mM Tris-HCl, pH 7.4, 100 mM NaCl, 6% (w/v) sucrose, 0.06% (w/v) Triton X-114. The samples were incubated for an additional 10 min at 30°C. Other additions to the assay medium, such as EGTA, Ca^{2+}, GTP, and azolectin liposomes were used in various combinations. Cloudy solutions were centrifuged for 5 min at 1000 $\times$ *g* at room temperature. The upper aqueous phases were treated with fresh 0.5% and then 2% (w/v) Triton X-114 solution at 4°C, loaded onto a sucrose cushion, as described above, incubated at 30°C for 5 min, and centrifuged. Aliquots of the separated phases were analyzed by SDS-PAGE (under reducing conditions) on 5% stacking and 7.5% or 12% resolving gels (Laemmli, 1970).

Preparation of AnxVI samples for infrared spectra

AnxVI was lyophilized and dissolved in ^2H_2O buffer containing 100 mM Tris-HCl, p^{2}H 7.4, 2 mM $CaCl_2$, and 2 mM caged-GTPγS, with or without PC/PS liposomes (2 mg/ml, 1:3 w/w). Formation of liposomes was obtained by hydrating the film of lipids with ^2H_2O buffer. The protein concentration was 100 μM. The p^{2}H was determined with a glass electrode and was corrected by a value of 0.4 (Glasoe and Long, 1960). Buffers without protein (100 mM Tris-HCl, p^{2}H 7.4, 2 mM $CaCl_2$ and 2.0 mM caged-GTPγS), with or without liposomes, were used to determine their infrared absorptions. All samples were freshly prepared and incubated for 5 min in the dark at room temperature before infrared measurement. The reaction-induced infrared spectra obtained after photorelease of GTPγS from caged-GTPγS were recorded under the same conditions as reported in Bandorowicz-Pikula et al. (1999).

Steady-state fluorescence measurements

The fluorescence of AnxVI (0–6 μM) and TNP-GTP (0–15 μM) were monitored at 25°C on a Fluorolog 3 spectrophotometer (Jobin Yvon Spex, Edison, NJ) with 3-nm slits for both excitation and emission. The assay media contained 50 mM Tris-HCl, pH 7.4, 20–50 mM NaCl, 2 mM $CaCl_2$, and as indicated were supplemented with azolectin (0.25 mg/ml) or PS/PC (0.25 mg/ml, 1:3 w/w) liposomes. Measurements were made in 5 $\times$ 5 mm cuvettes of 0.6 ml volume. TNP-GTP fluorescence emission spectra were recorded after excitation of samples at 415 nm, in a λ_{em} range from 500 to 600 nm and corrected as detailed in Bandorowicz-Pikula et al. (1999).

Fluorescence titrations with various nucleotide concentrations were monitored at λ_{em} 545 and 550 nm (λ_{ex} 415 nm). The specific fluorescence change (ΔF) of TNP-GTP, corresponding to the binding of nucleotide to AnxVI, was obtained by subtracting the nonspecific fluorescence measured in the presence of 2 mM GTP from the total fluorescence. To calculate the dissociation constant (K_d), the ΔF values were plotted versus TNP-GTP concentrations. The binding stoichiometry of TNP-GTP to AnxVI was determined from the mass action plot (Huang et al., 1998). Fluorescence resonance energy transfer (FRET) between protein Trp residues and nucleotide were measured after excitation of AnxVI Trp in the presence or absence of TNP-GTP. Samples were excited at 295 nm and emission spectra were recorded in the λ_{em} range from 305 to 580 nm. The emission and excitation slits were set at 2 and 3 nm, respectively.

CD spectra of AnxVI

Far-UV CD spectra of AnxVI or its N- and C-terminal fragments were recorded at 25°C on an AVIV CD spectrophotometer (AVIV Associates Inc., Lakewod, NJ) with a 450-W light source under an N_2 atmosphere. The protein spectra were recorded with a bandwidth of 1.0 nm, scan step 1.0 nm, and average time of 1.0 s. The optical pathlength of the quartz cuvette was 2 mm. The assay medium contained 0.2 mg protein/ml, 25 mM Tris-HCl, pH 7.4, 0.25 mg/ml azolectin and with 0–0.1 mM GTP.

RESULTS

GTP-stimulated ion channel activity of AnxVI

In our preliminary experiments we found that ATP/GTP evoked a stimulatory effect on the AnxVI-monolayer interaction at 3 μM Ca^{2+}, leading to an increase of surface pressure of the lipid monolayer. Therefore, we further tested the effect of GTP on the AnxVI/membrane interaction using planar azolectin membranes. By supplementing the assay medium with 2–20 nM AnxVI in the *cis* chamber, AnxVI

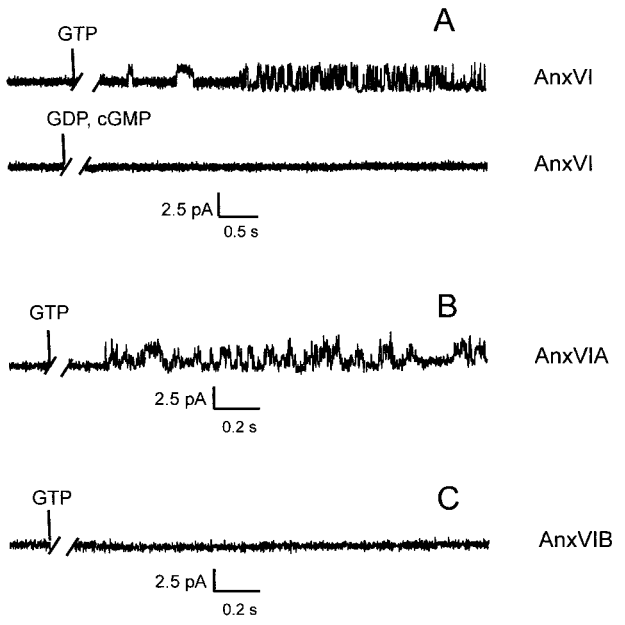

FIGURE 1 Ion channel activity of AnxVI in the presence of GTP. Single channel recordings of AnxVI (*A*), AnxVIA (*B*), and AnxVIB (*C*) incorporated into azolectin membranes were determined under symmetrical conditions, i.e., both chambers contained 10 mM Tris-Hepes, pH 7.4, 0.1 mM EGTA; 200 mM KCl, and either 4 mM GTP, GDP, GMP, or no nucleotide (as indicated in the figure). Current changes were induced by the addition of 20 nM protein into the *cis* chamber and recorded at a holding potential of +30 mV. The specific membrane capacitance was 150 pF. The time after the addition of GTP and appearance of channel activity was 10 min. This was faster when protein concentration was raised to 50 nM.

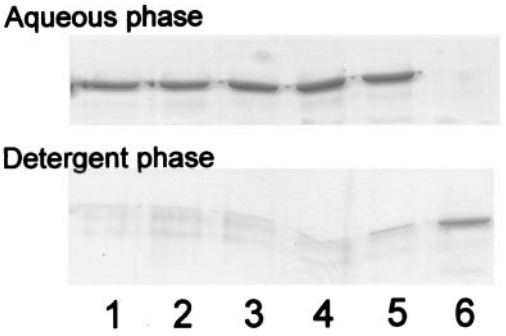

FIGURE 2 Partition of AnxVI between an aqueous and detergent phase. SDS-PAGE of peptide composition of aqueous (*upper panel*) or detergent (*lower panel*) phases. Additions were present during the partitioning process: *lane 1:* 1.0 mM EGTA; *lane 2:* 2 mM Ca^{2+}; *lane 3:* 1.0 mM EGTA + 4 mM GTP; *lane 4:* as lane 3 + azolectin liposomes; *lane 5:* 2 mM Ca^{2+}/azolectin liposomes + 4 mM GTP; *lane 6:* no additions. Except lane 6, where the pH of the assay medium was 3.0 (10 mM citrate buffer), the pH of media in lanes 1–5 was 7.4 (10 mM Tris-Hepes buffer).

was not incorporated into the lipid bilayer for 45 min at 22°C. To induce channel activity, the presence of GTP in the low millimolar concentration range was a prerequisite (Fig. 1 *A*). A single channel conductance (32.3 ± 1.6 pS, $n = 3$, under symmetric conditions, e.g., with 200 mM KCl in both chambers; current changes were induced by the addition of 20 nM protein into the *cis* chamber and recorded at different holding potentials from +60 mV to −30 mV) was observed, similar to that observed at low pH (Golczak et al., 2001). The GTP-induced ion channels were formed independently of the presence of Ca^{2+}. Moreover, addition of either GDP or cGMP, in the same concentration range as GTP, did not induce channel formation. Similar experiments performed on recombinant fragments of AnxVI indicated that the ion channel activity was impaired in the case of fragment AnxVIB (Fig. 1 *C*), while a channel activity similar to that of the whole molecule was measured in the case of AnxVIA (Fig. 1 *B*).

Interaction of AnxVI with membranes in the presence of GTP

A phase separation test using Triton X-114 indicated that AnxVI did not partition into the detergent hydrophobic phase in the presence of azolectin liposomes, GTP, Ca^{2+}, or combination of thereof (Fig. 2, *lanes* 1–5). Consequently, the interaction of AnxVI with azolectin membranes induced by GTP was not accompanied by a profound change in protein hydrophobicity. This was confirmed by incubating AnxVI at pH 3.0, which rendered AnxVI more hydrophobic (Golczak et al., 2001). Under these conditions, AnxVI penetrated the membrane hydrophobic region (Golczak et al., 2001) and partitioned into the detergent hydrophobic phase (Fig. 2, *lane* 6). Densitometric analysis of Fig. 2 revealed that <10% of the AnxVI was found in the detergent phase of lanes 1–5, but >90% of AnxVI was found in the detergent phase of lane 6.

Furthermore, CD spectra of AnxVI measured at pH 7.4 in the presence of Ca^{2+}/azolectin liposomes were indicative of only slight alterations of α-helix content of AnxVI occurring upon membrane binding in the presence of GTP. These alterations were characterized by the flattening of the CD minima located at λ 208 nm and at λ 222 nm (Fig. 3), suggesting a slight decrease of α-helix chain length (Yang et al., 1986).

Infrared spectra of AnxVI in the presence of GTP and lipids

The bottom trace in Fig. 4 shows a part of the infrared spectrum of 100 μM AnxVI in ^2H_2O buffer containing 100 mM Tris-HCl, p^{2}H 7.4, 2 mM $CaCl_2$. The 1652-cm^{-1} band was assigned to the amide-1 region, highly characteristic of α-helix structures (Byler and Susi, 1986; Surewicz et al., 1993; Goormaghtigh et al., 1994). The infrared spectrum of human recombinant AnxVI was identical to the infrared spectrum of native protein extracted from mammalian tissues (Bandorowicz-Pikula et al., 1999) and was similar to that of AnxV (Wu et al., 1998; Silvestro and Axelsen,

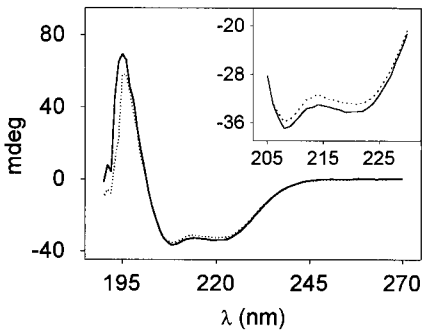

FIGURE 3 CD spectra of AnxVI in membrane-bound and soluble forms. Far UV-CD spectra of AnxVI (0.2 mg/ml) were recorded in buffer containing 50 mM Tris-HCl, pH 7.4, 2 mM Ca^{2+}, and 0.2 mg/ml azolectin liposomes in the absence (*solid line*) or presence (*dotted line*) of 0.1 mM GTP at 25°C. Unsmoothed and buffer-corrected spectra were averaged from at least five independent determinations. All results were consistent and varied by <5%. *Inset:* Same as main figure, indicating the region between λ 205–230 nm with two CD minima indicative of α-helix structures of AnxVI.

1999). The infrared spectra of N-terminal (Fig. 4, AnxVIA, *middle trace*) and C-terminal (Fig. 4, AnxVIB, *top trace*) fragments of AnxVI in the amide-1 region were indistinguishable from the infrared spectrum of whole AnxVI, suggesting that AnxVI and its fragments, AnxVIA and AnxVIB, had the same α-helix-reach secondary structures as expected from x-ray-derived structures of bovine (Avila-Sakar et al., 1998) and human recombinant AnxVI (Benz et al., 1996). This was also confirmed by comparing CD spectra of human recombinant proteins and AnxVI purified from porcine liver (results not shown). In the same type of experiments as described in Fig. 4, Ca^{2+}-PS/PC liposomes were used to explore GTP-induced interactions between AnxVI and lipids. The infrared spectrum of Ca^{2+}-PC/PS liposomes containing AnxVI (Fig. 5, *dashed line*) shows a

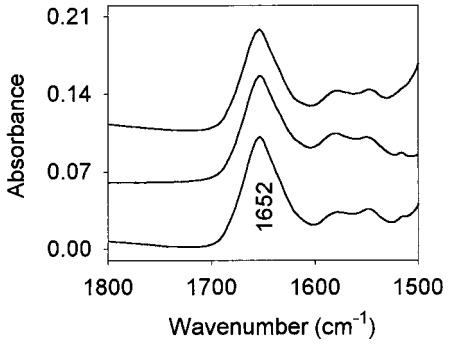

FIGURE 4 Infrared spectra of whole AnxVI and its N- (AnxVIA) and C-terminal (AnxVIB) fragments. Infrared spectra of whole AnxVI (*bottom trace*), AnxVIA (*middle trace*), and AnxVIB (*top trace*) in ^2H_2O buffer (7–8 mg protein ml^{-1} 100 mM Tris-HCl, pH 7.4, 2 mM $CaCl_2$) after subtraction of the infrared absorption of the buffer without protein. Each spectrum represented nine spectra that were averaged.

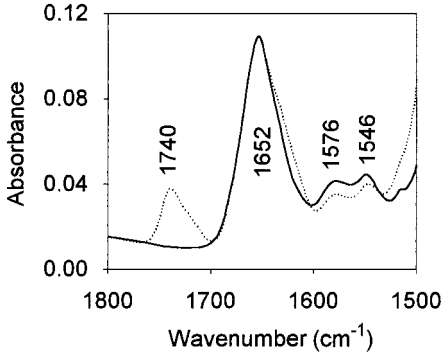

FIGURE 5 Infrared spectra of AnxVI with liposomes. Infrared spectra of AnxVI in the absence (*solid line*) or presence (*dashed line*) of Ca^{2+}-PC/PS liposomes before illumination of the sample with UV light. Each spectrum represented nine spectra that were averaged and corrected for buffer absorption. The maxima at 1652-cm^{-1} were normalized.

new component band at 1623 cm^{-1} that was absent in the infrared spectrum of AnxVI (Fig. 5, *solid line*). This was assigned to the serine moiety of Ca^{2+}-PC/PS liposomes, as evidenced by the presence of the 1623-cm^{-1} band in the infrared spectrum of Ca^{2+}-PC/PS liposomes (Fig. 6, *top trace*). The difference between the infrared spectrum of AnxVI and that of Ca^{2+}-PC/PS liposomes containing AnxVI (Fig. 6, *bottom trace*) revealed little alteration around 1667–1655 cm^{-1}, suggesting that only a small fraction of α-helical structures of AnxVI was affected upon lipid-binding, consistent with CD measurements (Fig. 3). The 1740-cm^{-1} band (Fig. 6, *bottom trace*) corresponded to the carbonyl groups of the ester moieties of Ca^{2+}-PC/PS liposomes measured in the presence of AnxVI. Its location and shape remained unaltered compared with the infrared

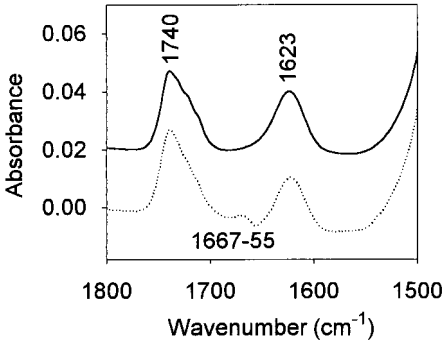

FIGURE 6 Difference infrared spectra of Ca^{2+}-PC/PS liposomes in the absence or presence of AnxVI. Infrared spectra of Ca^{2+}-PC/PS liposomes in the absence (*top trace*) or in the presence (*bottom trace*) of AnxVI, before illumination of the sample with UV light. Each spectrum represented nine spectra that were averaged and corrected for buffer absorption. In the bottom trace, the infrared spectrum of AnxVI was subtracted from the infrared spectrum of AnxVI with Ca^{2+}-PC/PS liposomes. Small alterations around 1667–1655 cm^{-1} reflected minor secondary structure changes in the protein molecule, while the 1740-cm^{-1} and 1623-cm^{-1} bands corresponded to lipid absorption.

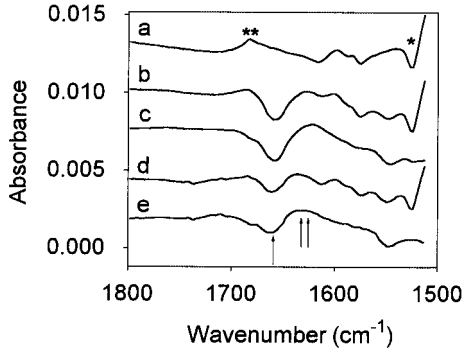

FIGURE 7 Structural changes evoked by binding of GTPγS to AnxVI. *Trace a:* averaged infrared difference spectrum induced by the photorelease of GTPγS from caged-GTPγS. *Trace b:* averaged infrared difference spectrum induced by the photorelease of GTPγS from caged-GTPγS in the presence of AnxVI. *Trace c:* infrared difference spectrum derived from spectrum represented by trace *b* after subtraction of infrared difference spectrum represented by trace *a*. *Trace d:* averaged infrared difference spectrum induced by the photorelease of GTPγS from caged-GTPγS in the presence of AnxVI and Ca^{2+}-PC/PS liposomes. *Trace e:* infrared difference spectrum derived from spectrum represented by trace *d* after subtraction of infrared difference spectrum of GTPγS (*trace a*). For each experiment, nine difference spectra were co-added and averaged. The AnxVI concentration was 7–8 mg protein ml^{-1} in ^2H_2O buffer containing 100 mM Tris-HCl, pH 7.4, 2 mM Ca^{2+}, 2 mM caged-GTPγS, with or without PS/PC liposomes (2 mg/ml), as indicated. **, the 1688–85-cm^{-1} band; *, the 1528–1527-cm^{-1} band; ↑, the 1656–1652-cm^{-1} band; ↑↑, the 1625–20-cm^{-1} band.

spectrum of pure Ca^{2+}-PC/PS liposomes (Fig. 6, *top trace*). After UV illumination, GTPγS was photoreleased from the inactive precursor, caged-GTPγS, initiating nucleotide binding to AnxVI. Trace *a* in Fig. 7 indicates the infrared difference spectrum of caged-GTPγS measured before and after UV illumination in the absence of AnxVI. The negative band at 1528–1527 cm^{-1} (*) and the positive band at 1688–1685 cm^{-1} (**) were attributed to the disappearance of the nitro group of photolabile GTPγS[1-(4,5-dimethoxy-2-nitrophenyl)-ethyl]) and the appearance of a carbonyl group of the photoproduct, respectively (Allin and Gerwert, 2001; Barth et al., 1997; Cepus et al., 1998). The measurement of their intensities served as a control for the amount of released GTPγS from caged compound. The difference infrared spectrum between that of nucleotide-unbound state (in the dark) and this of nucleotide bound to AnxVI (after photorelease of the nucleotide), indicated positive bands, associated with the effects of GTP binding to AnxVI, generating new structural features, while negative bands reflected the concomitant disappearance of initial structural features. The GTPγS-induced binding of nucleotide to AnxVI, in the absence of liposomes, produced a decrease of the 1656–1652-cm^{-1} (↑) and increase of the 1625–1620-cm^{-1} (↑↑) bands (Fig. 7, *trace b*), affecting α-helix and β-sheet structures, respectively. This was better evidenced on the infrared difference spectrum of AnxVI, after deduction of the infrared difference spectrum of caged-GTPγS, indicating only the effects of GTP binding to AnxVI (Fig. 7, *trace c*). In the presence of Ca^{2+}-PC/PS liposomes the same effects were observed, but their magnitude decreased by half (Fig. 7, *traces d* and *e*). A total of eight or nine amino acid residues were involved upon GTPγS binding to AnxVI in the absence of liposomes, while three or four amino acid residues were affected during GTPγS binding to AnxVI in the presence of Ca^{2+}-PC/PS liposomes. It is worth noting that the 3000–2800-cm^{-1} and 1200–1000-cm^{-1} regions of the infrared spectrum of AnxVI with liposomes and caged-GTPγS, where hydrocarbon chains and phosphate groups of lipids absorb, respectively, did not exhibit significant spectral changes caused by nucleotide binding to AnxVI associated with PC/PS liposomes in the presence of Ca^{2+}.

Characteristics of the binding of TNP-GTP to AnxVI

TNP-GTP, an extrinsic fluorescence probe for the GTP-binding proteins, is specifically competed by GTP in the millimolar concentration range (Randak et al., 1996; Gonzalo et al., 2000). The binding of TNP-GTP to AnxVI was optimal in the presence of Ca^{2+}-azolectin liposomes, as evidenced by an increase of the fluorescence emission of the GTP derivative and blue-shift by 20 nm of its emission maximum (Fig. 8 *A*). The K_d value of membrane-bound AnxVI for TNP-GTP in the presence of Ca^{2+}-azolectin liposomes was 1 μM, and its stoichiometry amounted to 1 (Table 1). Similar results were obtained in the presence of Ca^{2+}-PS/PC liposomes (data not shown). These values were in agreement with data obtained with TNP-ATP and nonfluorescent nucleotides (Bandorowicz-Pikula and Awasthi, 1997; Bandorowicz-Pikula et al., 1999).

The TNP-GTP binding to AnxVI was accompanied by FRET from AnxVI Trp residues to the nucleotide, as evidenced from an increase of the extrinsic fluorescence of TNP-GTP at λ_{em} 530 nm, determined for a fixed concentration of AnxVI and TNP-GTP concentrations ranging from 0 to 15 μM (Fig. 8 *B*). FRET was negligible in the absence of liposomes.

The two subcloned fragments of human recombinant AnxVI, corresponding to the N-terminal (AnxVIA) and C-terminal (AnxVIB) fragments of the protein, also bound TNP-GTP. AnxVIA revealed TNP-GTP binding properties similar to whole annexin (Table 1). However, AnxVIB was found to bind TNP-GTP with a 10-fold lower efficiency than AnxVI under optimal conditions (Table 1), consistent with the ion channel activity depicted in Fig. 1, *B* and *C*.

To follow the specificity of TNP-GTP binding to AnxVI, other nucleotides (GTP, GDP, cGMP) or guanosine were added and TNP-GTP fluorescence was determined. The concentration of TNP-GTP was 10 μM, corresponding to an occupancy of >90% of the binding sites in AnxVI (before addition of guanine nucleotides), assuming that the signal coming from bound TNP-GTP was not modified by the

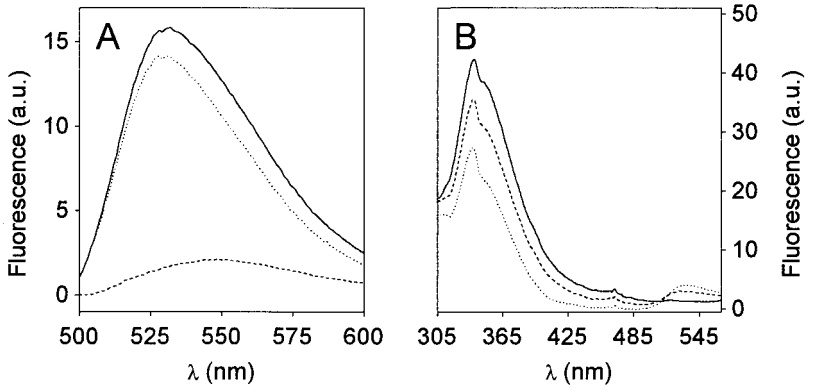

FIGURE 8 Binding TNP-GTP to AnxVI. (*A*) The extrinsic fluorescence of 5 μM TNP-GTP was measured in the absence of protein (*dashed curve*) and in the presence of 2 μM AnxVI (*solid curve*). The dotted curve represents the difference spectrum of TNP-GTP. Measurements were performed in the presence of 0.25 mg/ml azolectin liposomes and 2 mM Ca^{2+}. The spectra represent typical spectra chosen from at least three different experiments. The experimental error was <10%. (*B*) Quenching of the intrinsic fluorescence of AnxVI by TNP-GTP and FRET. Measurements were carried out in the presence of 1.5 μM AnxVI in 20 mM Tris-HCl buffer, pH 7.4, 50 mM NaCl, 2 mM Ca^{2+} and in the presence of azolectin liposomes (0.25 mg/ml). TNP-GTP was added to the following concentrations: none (*solid line*), 5 μM (*dashed line*), and 15 μM (*dotted line*). Samples were excited at λ_{exc} = 295 nm. Typical spectra chosen from three different are shown. They varied by <5%.

presence of the purine derivative. Under these conditions, TNP-GTP was released very efficiently from AnxVI by GTP (concentration of GTP for half-maximal release amounted to 4.2 mM) in contrast to GDP (maximal release was 25% in the presence of 10 mM nucleotide) or cGMP (no effect). ATP was as efficient as GTP in releasing TNP-GTP from AnxVI, pointing to the identity of GTP/ATP binding sites within the AnxVI molecule, as suggested earlier (Bandorowicz-Pikula et al., 2001).

DISCUSSION

Ion conductance measurements on AnxVI channels

At physiological pH, AnxVI formed voltage-dependent calcium-specific ion channels (Hofmann et al., 1997; Benz et al., 1996) in PS-enriched membranes that were inhibited by calcium channel antagonists, such as benzodiazepine derivatives (Kourie and Wood, 2000). In addition, nonspecific voltage-dependent ion channels, with a single channel conductance of ~24 pS in the presence of 50 mM CsCl were determined upon acidification of the assay medium (Golczak et al., 2001). Under our conditions, we were able to measure the ion channel activity of AnxVI at pH 7.4 only in the presence of GTP. In contrast to ion channels formed by AnxVI at acidic pH (Golczak et al., 2001), we did not observe any changes in protein hydrophobicity in the presence of GTP, as determined by the Triton X-114 partition experiment in which one may distinguish between integral and peripheral membrane proteins (Bordier, 1981). Moreover, the crystal structure of AnxVI revealed only discrete structural differences between the membrane-bound protein and AnxVI in solution (Benz et al., 1996; Avila-Sakar et al., 1998). In the membrane-bound form of AnxVI, the two halves of the molecule were coplanar with the membrane, but oriented differently (Avila-Sakar et al., 2000), suggesting a flexible arrangement of the molecule at the membrane surface. Such a flexible conformation of AnxVI may be regulated by GTP binding, pH, or other still unidentified ligands, resulting in various mechanisms of ion channel formation by AnxVI. The differences between AnxVIA and AnxVIB in GTP-induced ion channel activity and affinity for TNP-GTP are in line with this interpretation.

TABLE 1 Binding characteristics of TNP-GTP to human AnxVI, AnxVIA, and VIB in the presence of asolectin liposomes and Ca^{2+}

	Binding Monitored by Fluorescence*			Binding Monitored by Trp quenching†
Protein	λ_{em} Max.‡ (nm)	Fluorescence Increase§	K_d (μM)	Max. Quenching (%)
AnxVI	531 ± 1	×8.1	0.97 ± 0.11	34.7
AnxVIA	527 ± 2	×9.8	0.67 ± 0.16	31.5
AnxVIB	538 ± 2	×8.9	10.60 ± 2.71	—

*Fluorescence measurements of TNP-GTP were performed at the wavelength of maximum emission after excitation at 415 nm.
†Fluorescence measurements were performed at 339 nm after excitation at 295 nm.
‡The maximum emission wavelength of free TNP-GTP was 553 ± 1 nm.
§Related to the extrinsic fluorescence yield of free TNP-GTP.

Nucleotide binding of AnxVI in the presence of lipids

Only a small fraction of α-helical structures of AnxVI was affected during the addition of Ca^{2+}-PS/PC liposomes, as evidenced from infrared spectra of AnxVI. Further addition

of GTP indicated only minor structural alterations of membrane-bound AnxVI, as also probed by CD spectroscopy of AnxVI in the presence of Ca^{2+}-liposomes. The binding of nonhydrolyzable GTPγS to AnxVI induced very small structural changes, corresponding to eight or nine amino acid residues in the absence of liposomes or to three to four amino acid residues in the presence of Ca^{2+}-PS/PC liposomes, as indicated by infrared spectra, suggesting that the nucleotide-binding site overlapped the lipid-binding domain of AnxVI. No additional changes were observed in the infrared spectra of the CH- and phosphate-absorbing regions, consistent with the observation that GTP binding did not produce changes of protein hydrophobicity, as probed by the detergent phase separation experiment. Therefore, channel formation of AnxVI molecules, induced by GTP, was not accompanied by a significant penetration of AnxVI into the hydrophobic portion of the lipid bilayer. Alternatively, the lack of GTP-induced changes in the structure of lipids could reflect that ion conductance measurements monitored the activity of one single ion channel, while the population of AnxVI in the channel configuration was too small to be detected by spectroscopic and detergent partition methods. Despite the fact that the GTP-induced interactions between AnxVI and lipids remained very small, other investigators reported that purine nucleotides affected the interaction of annexins with membranes. Addition of cAMP or ATP altered the ion channel activity of AnxI and the aggregation between AnxI and chromaffin granules (Cohen et al., 1995). GTP reduced the number of events and conductance states, leading to well-defined Ca^{2+} channel activity of AnxV in the presence of liposomes (Arispe et al., 1996a). The presence of nucleotides modified the AnxVI binding to hepatocyte plasma membranes (Tagoe et al., 1994), and its ability to aggregate PS liposomes (Bandorowicz-Pikula and Pikula, 1998) and efficient hydrolysis of GTP by AnxVII occurred in the presence of Ca^{2+}/liposomes (Caohuy et al., 1996).

Determination of nucleotide-binding parameters by fluorescence

Fluorescent analogs of nucleotides permitted the determination of the nucleotide-binding parameters of AnxVI (Bandorowicz-Pikula and Awasthi, 1997) and other unrelated proteins (Randak et al., 1996; Han et al., 1998). AnxVI bound TNP-GTP with a stoichiometry of 1 and high affinity (K_d was 1 μM) in a specific protein domain located within a FRET distance between Trp residues of AnxVI and the TNP-GTP-binding site. Nucleotide binding was optimal in the presence of liposomes and Ca^{2+}, suggesting that AnxVI, under these conditions, was in the best configuration to bind TNP-GTP. The affinity of TNP-GTP to AnxVI was fivefold higher than that of nonfluorescent nucleotide to AnxVI. A similar enhancement of affinity was observed in the case of TNP-ATP for porcine liver AnxVI (Bandorowicz-Pikula and Awasthi, 1997) or of TNP-ATP/TNP-ADP for the simian virus SV40 large tumor antigen (Huang et al., 1998).

Comparison with other peptides forming ion channels

To understand the mechanism of ion channel formation, it is valuable to compare results obtained for other annexins and unrelated ion channel-forming proteins and peptides. It was proposed that GTP-binding to AnxV stabilizes the cation channel to a reduced number of conformations that have well-defined open and closed states and conductance levels, while addition of ATP or Zn^{2+} produced distinct effects (Arispe et al., 1996a). The β-amyloid peptide formed cation-selective channels with wide range of conductance ranging from 40 to 4000 pS, and it was suggested that different polymeric states could be responsible for the different conductance states (Arispe et al., 1996b). Therefore, the existence of various conductances in all these channels could be associated with the interconversion between distinct oligomeric states. Alternatively, it is believed that the general mechanism of cellular toxicity evoked by amyloid peptides is related to their specific processing, e.g., conformational changes leading to the formation of partially folded intermediate. This step involves conversion of α-helix to a β-pleated sheet structure (Kourie, 2001; Kourie and Henry, 2001), and it was observed for Alzheimer's β-amyloid 40-residue-long peptide, human 37-residue-long peptide amylin from islets of Langerhans, and prion peptide PrP106–126 derived from a pathogenic form of cellular prion protein associated with several diseases such as scrapie, Kuru disease, Creutzfeldt-Jakob disease, and bovine spongiform encephalopathy (Kawahara et al., 2000). It is suggested that the structural changes may trigger protein nucleation and polymerization, cause aggregation (Kourie and Henry, 2001), and are associated with the formation of ion channels across cellular membranes (Kawahara et al., 2000). It is possible that the essential feature of pathogenic channel-forming peptides, such as Alzheimer's β-amyloid peptides, amylin, and prion peptides is to adopt the β-pleated sheet structure in combination with hydrophobic domains on the cell membrane (Prusiner et al., 1998), relatively depleted of cholesterol. Indeed, it was observed that water-soluble cholesterol (polyoxyethanyl cholesteryl sabacate) substantially decreased the fraction of acidic phospholipids in membranes and inhibited incorporation of amyloid peptides into membranes (Kawahara et al., 2000). In the case of GTP-induced ion channels formed by AnxVI at neutral pH, these interconversions were not accompanied with significant changes of hydrophobicity or secondary structure of the protein. Moreover, in stimulated smooth muscle cells AnxVI was found associated with glycosphingolipid- and cholesterol-enriched membrane microdomains (Babiychuk and Draeger, 2000), and in in vitro experiments cholesterol stimulated binding of AnxVI to membranes

(Ayala-Sanmartin, 2001). It remains to be elucidated whether cholesterol may also modify the ion channel activity of AnxVI at neutral pH. However, it was described for AnxVI (Golczak et al., 2001), AnxV (Kohler et al., 1997; Isas et al., 2000; Sopkova-De Oliveira Santos et al., 2000), and AnxXII (Cartailler et al., 2000; Isas et al., 2000) that formation of low pH-induced channels by these annexins is associated with changes of their hydrophobicity, rearrangement of secondary structure, and oligomerization, pointing to the different mechanism of formation of ion channels by the annexin molecules at low pH and those induced by GTP at neutral pH.

CONCLUDING REMARKS

A possible physiological significance of our observations is underlined by the fact that GTP induced the formation of ion channels by AnxVI molecules in a millimolar concentration range of nucleotide. The differences between the channel properties of AnxVI at acidic and neutral pH could originate from distinct protein/protein interactions and domain flexibilities. Such ligand-binding induced structural alterations, and their distinct molecular responses imply that AnxVI could function as a biosensor sensitive to GTP, pH, ions, and eventually to some pathological states where cellular signal transduction processes, energy metabolism, and/or ion homeostasis are affected (Bandorowicz-Pikula et al., 2001).

We thank Professor R. Huber from the Max-Planck-Institut fur Biochemie, Martinsried, Germany, for providing cDNA for human AnxVI, and Professor R. Donato from Universita di Perugia, Italy, for sending *E. coli* transformed with AnxVI cDNA. The black lipid membrane conductance measurements were performed in the Laboratory of Intracellular Ion Channels at the Nencki Institute of Experimental Biology. We express our gratitude to Dr. Patrick Groves from the Nencki Institute of Experimental Biology, Warsaw, Poland, for critical reading of the manuscript.

This work was supported by State Committee for Scientific Research Grants 3 PO4A 007 22 and 6 P04A 039 21, and a grant from CNRS.

REFERENCES

Allin, C., and K. Gerwert. 2001. Ras catalyzes GTP hydrolysis by shifting negative charges from γ- to β-phosphate as revealed by time-resolved FTIR difference spectroscopy. *Biochemistry.* 40:3037–3046.

Arispe, N., H. B. Pollard, and E. Rojas. 1996b. Zn^{2+} interaction with Alzheimer amyloid protein calcium channels. *Proc. Natl. Acad. Sci. U.S.A.* 93:1710–1715.

Arispe, N., E. Rojas, B. R. Genge, L. N. Y. Wu, and R. E. Wuthier. 1996a. Similarity in calcium channel activity of annexin V and matrix vesicles in planar lipid bilayers. *Biophys. J.* 71:1764–1775.

Avila-Sakar, A. J., C. E. Creutz, and R. H. Kretsinger. 1998. Crystal structure of bovine annexin VI in a calcium-bound state. *Biochim. Biophys. Acta.* 1387:103–116.

Avila-Sakar, A. J., R. H. Kretsinger, and C. E. Creutz. 2000. Membrane-bound 3D structures reveal the intrinsic flexibility of annexin VI. *J. Struct. Biol.* 130:54–62.

Ayala-Sanmartin, J. 2001. Cholesterol enhances phospholipid binding and aggregation of annexins by their core domain. *Biochem. Biophys. Res. Commun.* 283:72–79.

Babiychuk, E. B., and A. Draeger. 2000. Annexins in cell membrane dynamics. Ca^{2+}-regulated association of lipid microdomains. *J. Cell Biol.* 150:1113–1124.

Bandorowicz-Pikula, J., and Y. C. Awasthi. 1997. Interaction of annexins IV and VI with ATP: an alternative mechanism by which a cellular function of these calcium- and membrane-binding proteins is regulated. *FEBS Lett.* 409:300–306.

Bandorowicz-Pikula, J., R. Buchet, and S. Pikula. 2001. Annexins as nucleotide-binding proteins: facts and speculations. *BioEssays.* 23: 170–178.

Bandorowicz-Pikula, J., and S. Pikula. 1998. Modulation of annexin VI-driven aggregation of phosphatidylserine liposomes by ATP. *Biochimie.* 80:613–620.

Bandorowicz-Pikula, J., A. Wrzosek, M. Danieluk, S. Pikula, and R. Buchet. 1999. ATP-binding site of annexin VI characterized by photochemical release of nucleotide and infrared difference spectroscopy. *Biochem. Biophys. Res. Commun.* 263:775–779.

Barth, A., J. E. T. Corie, M. J. Gradwell, Y. Maeda, W. Mantele, T. Meier, and D. R. Trentham. 1997. Time-resolved infrared spectroscopy of intermediates and products from photolysis of 1-(2-nitrophenyl)ethyl phosphates: reaction of the 2-nitrosophenone by product with thiols. *J. Am. Chem. Soc.* 119:4149–4159.

Benz, J., A. Bergner, A. Hofmann, P. Demange, P. Gottig, S. Liemann, R. Huber, and D. Voges. 1996. The structure of recombinant human annexin VI in crystals and membrane-bound. *J. Mol. Biol.* 260:638–643.

Bordier, C. 1981. Phase separation of integral membrane proteins in Triton X-114 solution. *J. Biol. Chem.* 256:1604–1607.

Burger, A., R. Berendes, D. Voges, R. Huber, and P. Demange. 1993. A rapid and efficient purification method for recombinant annexin V for biophysical studies. *FEBS Lett.* 329:25–28.

Byler, D. M., and H. Susi. 1986. Examination of the secondary structure of proteins by deconvolved FTIR spectra. *Biopolymers.* 25:469–487.

Calvo, M., A. Pol, A. Lu, D. Ortega, M. Pons, J. Blasi, and C. Enrich. 2000. Cellubrevin is present in the basolateral endocytic compartment of hepatocytes and follows the transcytotic pathway after IgA internalization. *J. Biol. Chem.* 275:7910–7917.

Caohuy, H., M. Srivastava, and H. B. Pollard. 1996. Membrane fusion protein synexin (annexin VII) as a Ca^{2+}/GTP sensor in exocytotic secretion. *Proc. Natl. Acad. Sci. U.S.A.* 93:10797–10802.

Cartailler, J. P., H. T. Haigler, and H. Luecke. 2000. Annexin XII E105K crystal structure: identification of a pH-dependent switch for mutant hexamerization. *Biochemistry.* 39:2475–2483.

Cepus, V., C. Ulbrich, C. Allin, A. Trouiller, and K. Gerwert. 1998. Fourier transform infrared photolysis studies of caged-compounds. *Methods Enzymol.* 291:223–245.

Chow, A., A. J. Davis, and D. J. Gawler. 2000. Identification of a novel protein complex containing annexin VI, Fyn, Pyk2, and the $p120^{GAP}$ C2 domain. *FEBS Lett.* 469:88–92.

Cohen, B. E., G. Lee, N. Arispe, and H. B. Pollard. 1995. Cyclic 3′-5′-adenosine monophosphate binds to annexin I and regulates calcium-dependent membrane aggregation and ion channel activity. *FEBS Lett.* 377:444–450.

Glasoe, P. K., and F. A. Long. 1960. Use of glass electrodes to measure acidities in deuterium oxide. *J. Phys. Chem.* 64:188–190.

Golczak, M., A. Kicinska, J. Bandorowicz-Pikula, R. Buchet, A. Szewczyk, and S. Pikula. 2001. Acidic pH-induced folding of annexin VI is a prerequisite for its insertion into lipid bilayers and formation of ion channels by the protein molecules. *FASEB J.* 15:1083–1085.

Gonzalo, P., B. Sontag, J. P. Lavergne, J. Jault, and J. P. Reboud. 2000. Evidence for a second nucleotide binding site in rat elongation factor eEF-2 specific for adenylic nucleotides. *Biochemistry.* 39:13558–13564.

Goormaghtigh, E., V. Cabiaux, and J. M. Ruysschaert. 1994. Determination of soluble and membrane protein structure by Fourier transform infrared spectroscopy. I. Assignments and model compounds. *In* Phys-

ical Methods in the Study of Biomembranes. H. J. Hilderson and G. B. Ralston, editors. Plenum Press, New York. 23:329–362.

Grewal, T., J. Heeren, D. Mewawala, T. Schnitgerhans, D. Wendt, G. Salomon, C. Enrich, U. Beisiegel, and S. Jackle. 2000. Annexin VI stimulates endocytosis and is involved in the trafficking of low density lipoprotein to the prelysosomal compartment. *J. Biol. Chem.* 275: 33806–33813.

Han, Y., H. Malak, A. G. Chaudhary, M. D. Chordia, D. G. Kingston, and S. Bane. 1998. Distances between the paclitaxel, colchicine, and exchangeable GTP binding sites on tubulin. *Biochemistry.* 37:6636–6644.

Hofmann, A., J. Benz, S. Liemann, and R. Huber. 1997. Voltage dependent binding of annexin V, annexin VI and annexin VII-core to acidic phospholipid membranes. *Biochim. Biophys. Acta.* 1330:254–264.

Huang, S. G., K. Weisshart, and E. Fanning. 1998. Characterization of the nucleotide binding properties of SV40 T antigen using fluorescent 3′(2′)-*O*-(2,4,6-trinitrophenyl)adenine nucleotide analogues. *Biochemistry.* 37:15336–15344.

Isas, J. M., J. P. Cartailler, Y. Sokolov, D. R. Patel, R. Langen, H. Luecke, J. E. Hall, and H. T. Haigler. 2000. Annexins V and XII insert into bilayers at mildly acidic pH and form ion channels. *Biochemistry.* 39:3015–3022.

Kawahara, M., Y. Kuroda, N. Arispe, and E. Rojas. 2000. Alzheimer's β-amyloid, human islet amylin, and prion protein fragment evoke intracellular free calcium elevations by a common mechanism in a hypothalamic GnRH neuronal cell line. *J. Biol. Chem.* 275:14077–14083.

Kirsch, T., G. Harrison, E. E. Golub, and H. D. Nah. 2000. The roles of annexins and types II and X collagen in matrix vesicle-mediated mineralization of growth plate cartilage. *J. Biol. Chem.* 275:35577–35583.

Kohler, G., U. Hering, O. Zschornig, and K. Arnold. 1997. Annexin V interaction with phosphatidylserine-containing vesicles at low and neutral pH. *Biochemistry.* 36:8189–8194.

Kourie, J. I. 2001. Mechanisms of prion-induced modifications in membrane transport properties: implications for signal transduction and neurotoxicity. *Chem. Biol. Interact.* 138:1–26.

Kourie, J. I., and C. L. Henry. 2001. Protein aggregation and deposition: implications for ion channel formation and membrane damage. *Croat. Med. J.* 42:359–374.

Kourie, J. I., and H. B. Wood. 2000. Biophysical and molecular properties of annexin-formed channels. *Prog. Biophys. Mol. Biol.* 73:91–134.

Laemmli, U. K. 1970. Cleavage of structural proteins during the assembly of the head of bacteriophage T4. *Nature (Lond.).* 227:680–685.

Michaely, P., A. Kamal, R. G. Anderson, and V. Bennett. 1999. A requirement for ankyrin binding to clathrin during coated pit budding. *J. Biol. Chem.* 274:35908–35913.

Ortega, D., A. Pol, M. Biermer, S. Jackle, and C. Enrich. 1998. Annexin VI defines an apical endocytic compartment in rat liver hepatocytes. *J. Cell Sci.* 111:261–269.

Pons, M., T. Grewal, E. Rius, T. Schnitgerhans, S. Jackle, and C. Enrich. 2001a. Evidence for the involvement of annexin 6 in the trafficking between the endocytic compartment and lysosomes. *Exp. Cell Res.* 269:13–22.

Pons, M., G. Ihrke, S. Koch, M. Biermer, A. Pol, T. Grewal, S. Jackle, and C. Enrich. 2000. Late endocytic compartments are major sites of annexin VI localization in NRK fibroblasts and polarized WIF-B hepatoma cells. *Exp. Cell Res.* 257:33–47.

Pons, M., F. Tebar, M. Kirchhoff, S. Peiro, I. de Diego, T. Grewal, and C. Enrich. 2001b. Activation of Raf-1 is defective in annexin 6 overexpressing Chinese hamster ovary cells. *FEBS Lett.* 501:69–73.

Prusiner, S. B., M. R. Scott, S. J. DeArmond, and F. E. Cohen. 1998. Prion protein biology. *Cell.* 93:337–348.

Randak, C., P. Neth, E. A. Auerswald, I. Assfalg-Machleidt, A. A. Rosher, H.-B. Hadorn, and W. Machleidt. 1996. A recombinant polypeptide model of the second predicted nucleotide binding fold of the cystic fibrosis transmembrane conductance regulator is a GTP-binding protein. *FEBS Lett.* 398:97–100.

Schmitz-Peiffer, C., C. L. Browne, J. H. Walker, and T. J. Biden. 1998. Activated protein kinase C alpha associates with annexin VI from skeletal muscle. *Biochem. J.* 330:675–681.

Silvestro, L., and P. H. Axelsen. 1999. Fourier transform infrared linked analysis of conformational changes in annexin V upon membrane binding. *Biochemistry.* 38:113–121.

Sopkova-De Oliveira Santos, J., S. Fischer, C. Guilbert, A. Lewit-Bentley, and J. C. Smith. 2000. Pathway for large-scale conformational change in annexin V. *Biochemistry.* 39:14065–14074.

Surewicz, W. K., H. H. Mantsch, and D. Chapman. 1993. Determination of protein secondary structure by Fourier transform infrared spectroscopy: a critical assessment. *Biochemistry.* 32:389–394.

Tagoe, C. E., C. M. Boustead, S. J. Higgins, and J. H. Walker. 1994. Characterization and immunolocalization of rat liver annexin VI. *Biochim. Biophys. Acta.* 1192:272–280.

Wu, F., A. Gericke, C. R. Flach, T. R. Mealy, B. A. Seaton, and R. Mendelsohn. 1998. Domain structure and molecular conformation in annexin V/1,2-dimyristoyl-*sn*-glycero-3-phosphate/Ca^{2+} aqueous monolayers: a Brewster angle microscopy/infrared reflection-absorption spectroscopy study. *Biophys. J.* 74:3278–3281.

Yang, J.-T., C.-S. Wu, and H. M. Martinez. 1986. Calculation of protein conformation from circular dichroism. *Methods Enzymol.* 130:208–269.

Zampighi, G. A., J. E. Hall, and M. Kreman. 1985. Purified lens junctional protein forms channels in planar lipid films. *Proc. Natl. Acad. Sci. U.S.A.* 82:8468–8472.